Protection behaviour of surface films formed on AZ91D magnesium alloy in nitrogen/1,1,1,2-tetrafluoroethane atmospheres

Article *in* Metals and Materials International · July 2014

DOI: 10.1007/s12540-014-4005-2

CITATIONS
5

READS
42

5 authors, including:

J.M Gómez de Salazar
Complutense University of Madrid
204 PUBLICATIONS **1,076** CITATIONS

SEE PROFILE

Irene Garcia Cano
University of Barcelona
267 PUBLICATIONS **1,064** CITATIONS

SEE PROFILE

Jose Maria Guilemany
University of Barcelona
1,515 PUBLICATIONS **5,899** CITATIONS

SEE PROFILE

Met. Mater. Int., Vol. 20, No. 4 (2014), pp. 613~618
doi: 10.1007/s12540-014-4005-2

Protection Behaviour of Surface Films Formed on AZ91D Magnesium Alloy in Nitrogen/1,1,1,2-Tetrafluoroethane Atmospheres

M. I. Barrena[1,*], J. M. Gómez de Salazar[1], J. M. Vázquez[1], I. García-Cano[2], and J. M. Guilemany[2]

[1]Universidad Complutense de Madrid,Departamento de Ciencia de los Materiales e Ingeniería Metalúrgica, Facultad de Ciencias Químicas. Av. Complutense s/n, 28040 Madrid, Spain
[2]Universitat de Barcelona, Centre de Projecció Tèrmica (CPT), Facultat de Química, Martí i Franquès 1, 08028 Barcelona, Spain

(received date: 24 April 2013 / accepted date: 30 October 2013)

Protective surface coatings on an AZ91D magnesium alloy were formed in an atmosphere mixture of nitrogen and 1,1,1,2-tetrafluoroethane (HFC-134a). The surface composition and microstructure were characterized using X-ray diffraction analysis and scanning electron microscopy, respectively. The cross-section morphologies of the coatings show that an increase in conversion time results in an increase in the continuity and compactness of the coating generated on the surface of the AZ91D alloy. The corrosion resistance tests performed by immersion into 3.5% NaCl solutions were investigated by electrochemical measurements. The results showed that the coated samples had higher corrosion resistance than the un-coated alloy. On the other hand, the corrosion density of the coated samples decreased by increasing the conversion time by about two orders of magnitude, compared with the un-coated samples. This behaviour is attributed to the formation of a protective surface film constituted mainly for MgF_2, together with other phases. The nature of these phases depends on the process conditions.

Keywords: magnesium alloy, surface film, corrosion, protection, microstructure

1. INTRODUCTION

Magnesium and its alloys are in demand in many industry applications due to their good properties [1]. However, their applications are still limited during service due to the extreme reactivity between magnesium and oxygen [2] and the poor corrosion resistance in particular in chloride containing solutions [3-7]. The poor corrosion behaviour of Mg alloys results from the high intrinsic dissolution tendency of magnesium, which is only inhibited by the corrosion product film that forms on the alloy surface. This protective film breaks due to the anodic and cathodic partial reactions taking place predominately on the Mg metal surface [8].

Therefore, it is necessary to protect these alloys in aggressive environments. Many efforts have been devoted to improving the anti-corrosion performance of magnesium alloys through the formation of favourable intermetallics [9-11], producing protective surface films [4,12-14] or modifiying the oxide layer on the surface [15]. Some coating technologies have been considered to be an effective way of controlling and reducing corrosion rates [16]. However, one of the main disadvantages in these processes is the toxicity of precursors such as SF_6 gas mixture. This gas can form a thin, coherent and stable film on the melt surface of Mg [17,18], but it has become recognized as a high greenhouse effect gas [19]. 1,1,1,2-Tetrafluoroethane (CF_3CH_2F, HFC-134a) has been developed for magnesium melt protection [20-22]. Therefore, HFC-134a is a good candidate for the replacement of SF_6.

Studies on reduction or inhibition of the oxidation of molten magnesium and its alloys in air using HFC-134a gas mixture are available in the literature [23-25]. However, this work investigates the generation of a protective surface film leaving the substrate (Mg alloys) in a solid state with using a N_2/HFC-134a gas mixture. The aim of the present work is to generate and characterize films on the AZ91D alloy surface using as precursors a mixture of nitrogen and 1,1,1,2-tetrafluoroethane. The characterization of the films obtained was investigated from the point of view of the microstructural and oxidation resistance.

2. EXPERIMENTAL PROCEDURE

The material used for the investigation was a commercial as-cast AZ91D magnesium alloy with a nominal composition (wt%) of Al 8.66, Zn 0.58, Mn 0.20, Si 0.019, Ni 0.008,

*Corresponding author: ibarrena@quim.ucm.es

Cu 0.003, Fe 0.0021 and Mg balance. The as-cast sheet was cut into samples with dimensions of 20×20×3 mm^3. Before exposure to the mixture gas, the samples were ground down to a 600 grit silicon carbide paper and cleaned in acetone followed by air drying. In order to form a surface coating on the AZ91D, thermal treatments were carried out at 550 ℃ during a conversion time of between 30 and 90 min. The chemical composition of both gases HFC-134a and technique N_2 was ≥99.998% pure. The furnace atmosphere was filled by N_2 containing 2% of HFC-134a and was controlled by flow meters.

Surface and cross section morphologies of the coating obtained were examined by scanning electron microscopy (JEOL 6400 operating at 20 kV). The main phases in the coating were detected using X-ray diffraction measurements (Philips X'Pert PD P3040 diffractometer with a CuKα source at 40 kV and 40 mA) and X-ray induced photoelectron spectroscopy (Perkin-Elmer 5400 ESCA Series attached with a 15 kV X-ray gun).

Potentiodynamic polarization experiments were performed in a three-electrode cell, using a platinum foil as counter electrode, an Ag/AgCl (satured KCl) electrode as a reference electrode and AZ91D or coated-AZ91D as a working electrode, which were covered with cold setting resin exposing an area of 1 cm^2 in a 3.5 wt% NaCl aerated solution (pH 6.84). Tests were carried out using a scanning rate of 1 mVs^{-1}. The corrosion potential and intensity were calculated from the polarization curves. All electrochemical measurements were repeated more than three times at 25 ℃ using an Amel model 2049 potentiostat for better reproducibility. The surface morphology and chemical composition of the phases were investigated after the corrosion tests.

3. RESULTS AND DISCUSSION

Both surface microstructure and chemical composition of the substrate change when it is exposed to temperature in a mixture gas. The process conversion time exerted an influence on the morphology of the surface film. Figure 1 shows the SEM images of the surface of AZ91D magnesium alloy after exposure to nitrogen containing a 2 wt% HFC-134a at 550 ℃ for times ranging from 30 to 90 min. It is clear that the surface morphology varies with the process time.

After exposure to the mixture gas during 30 min (Fig. 1a), the surface of substrate alloy was rough and contained numerous discontinuities, which indicated that the surface film will not provide effective protection to the substrate. Increasing the time to 60 min (Fig. 1b), the surface morphology is flatter and a smoother surface film could be seen on the surface of the AZ91D magnesium alloy. When the time was increased to 90 min a uniform and compact protective surface film

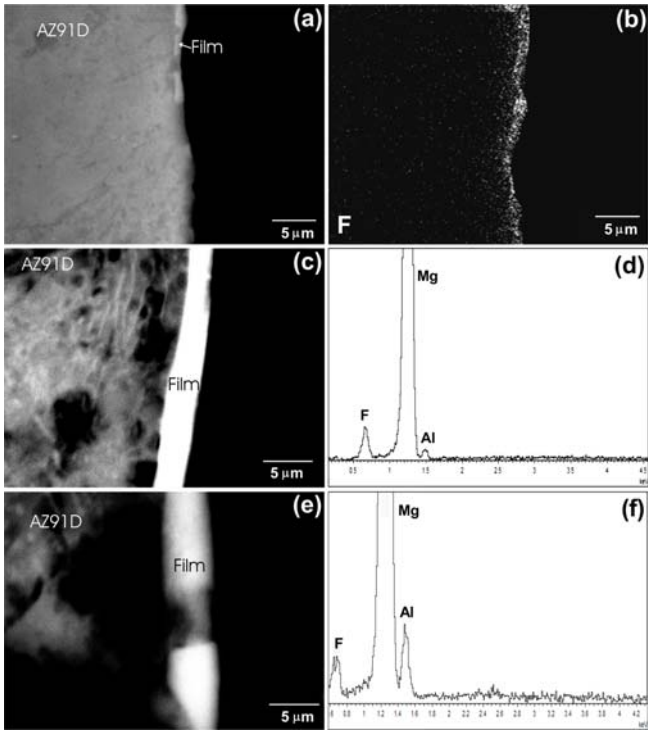

Fig. 2. Cross-sectional morphology and analysis of coated AZ91D magnesium alloy samples in N_2/2% HFC-134a gas mixture at 550℃, obtained for different conversion time: (a) SEM image and (b) energy spectrum image of F of sample obtained for 30 min; (c) SEM image and (d) EDS spectrum of sample obtained for 60 min; (e) SEM image and (f) EDS spectrum of sample obtained for 90 min.

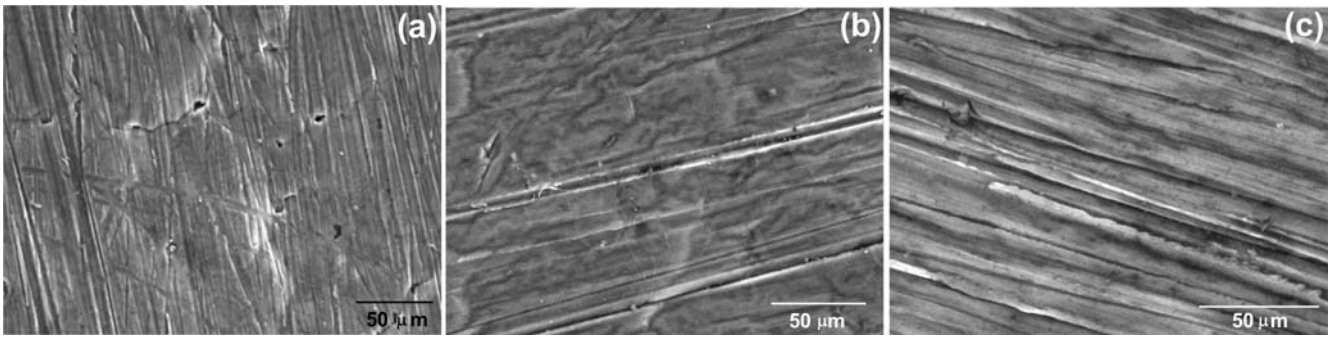

Fig. 1. SEM micrographs of the surface film under the atmosphere of N_2 containing 2% HFC-134a at 550℃ formed on AZ91D magnesium alloy for (a) 30 min, (b) 60 min and (c) 90 min.

(Fig. 1c) can clearly be observed. Analysing the cross-section morphology of the coating, we confirmed that the increase in conversion time results in an increase in the continuity and compactness of the coating generated on the surface of the AZ91D alloy. As can be seen from Fig. 2, the thickness of the surface film was estimated to be about 1-1.5 μm for 40 min and about 2-2.7 μm for 60 min. These thickness increased up to 5 μm for the longest time used. Good adhesion between the coating and the substrate is seen without a visible boundary in some cases, which is due to the fact that the coating is growing on the substrate by chemical conversion. However, discontinuities on the coating can be observed in the condition of the longest time. It seems that a part of the film had been dissolved. XRD analysis was used to analyse the surface composition change associated with these microstructures. It can be seen from Fig. 3 that the reaction products in the surface film varied with the conversion time. When the time used is between 30 and 60 min, the surface film consisted of MgO, MgF_2 and nitride of Mg and Al (Fig. 3a). The Mg peak may be caused by the X-ray radiation penetrating the thin film into the substrate alloy. The phases detected in these films are associated with the thermodynamic values of reaction. Mg and Al react with F_2, N_2 and O_2 contained in the mixture gas at 550 °C, with negative ΔG to these processes. As the time increases the no AlN was detected likely because the amount of this phase is too low to be detected by X-ray. However, the formation at a long conversion time of a new phase, AlF_3, is detected on the coating together with the phases detected for short conversion times. This phase (AlF_3) is water soluble so it could explain the presence on the film of gaps which form during the metallographic preparation process.

In order to confirm the presence of minor phases, the surface of all the films formed on AZ91D alloy were examined

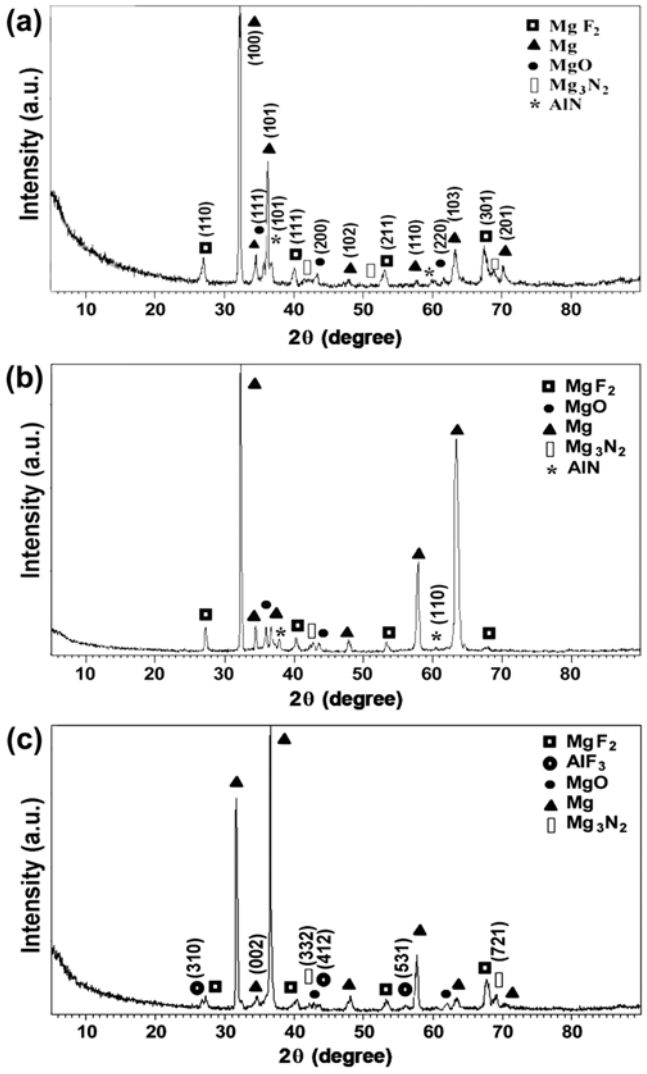

Fig. 3. XRD patterns of the film formed on AZ91D magnesium alloy samples after exposure to the atmosphere of N_2 containing 2% HFC-134-a for (a) 30 min, (b) 60 min and (c) 90 min.

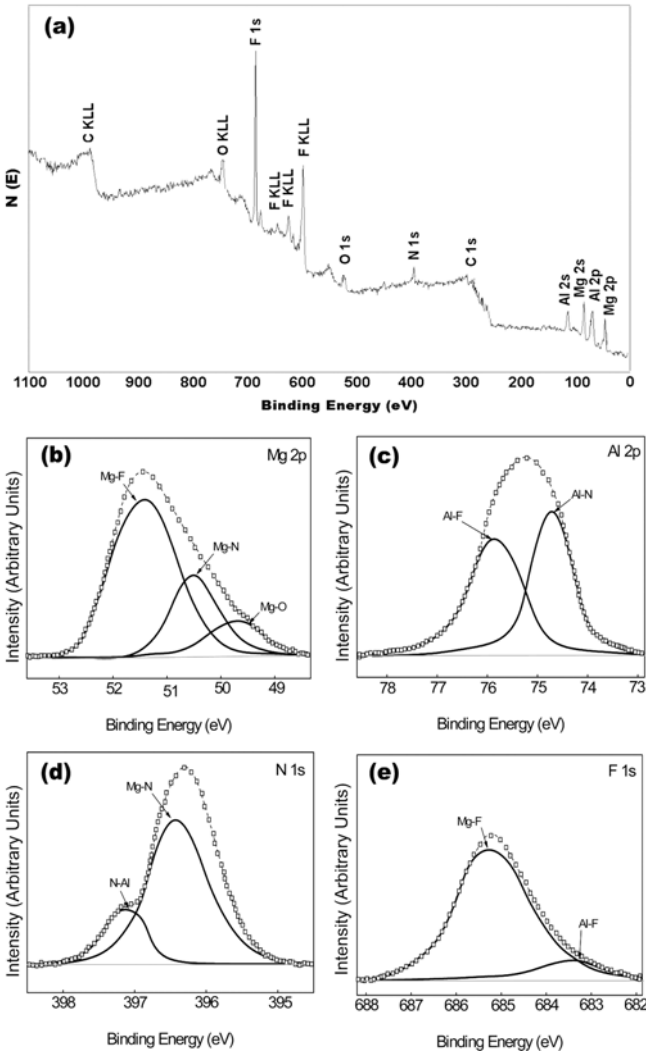

Fig. 4. XPS spectra of surface film formed on AZ91D alloy in N_2 containing 2% HFC-134-a for 30 min. (a) whole survey spectra, (b) Mg 2p, (c) Al 2p (d) N 1s and (e) F 1s.

Table 1. Element composition of the surface films formed on magnesium alloy after exposure to N_2 containing a 2 wt% HFC-134a for different conversion time at 550 ℃

Element	30 min	60 min	90 min
F	53.33	56.38	53.34
Mg	37.38	38.04	39.27
N	4.82	1.95	3.48
Al	2.77	3.00	3.44
O	1.70	0.63	0.47

by XPS. Figure 4a shows the XPS spectrum of the surface film formed for 30 min in a protective atmosphere of N_2 containing 2% HFC-134a. Based on the integrated peak intensity and taking into account the atomic sensibility factor, the elemental compositions of the film formed under different conversion times are shown in Table 1. The surface films consisted of magnesium, fluorine, aluminium, nitrogen and oxygen, which is in agreement with the results determined by X-ray. It can be seen that the content of magnesium and fluorine did not change significantly. The chemical structures of the films were determined by examining the Mg 2p, Al 2p, N 1s and F 1s core levels. Figure 4b gives the Mg 2p photoelectron spectrum. It can be deconvoluted into three components assigned to Mg-F (51.3 eV), Mg-N (50.5 eV) and Mg-O (49.7 eV) bonding. The existence of the last one confirms the extremely high chemical affinity of the magnesium with the oxygen. However, since the intensity of the peak at 49.7 eV was lower than that of the peak at 51.3 eV, it could be deduced that the content of MgO in the film was very small. The Al 2p state in Fig. 4c shows the peak shift due to nitride and fluoride formation at 74.6 eV and 75.9 eV, respectively. According to the N 1s spectrum (Fig. 4d), nitrogen presented in two chemical states. The lower binding energy peak at 397.2 eV was assigned to AlN and the higher binding energy peak at 396.4 eV was attributed to Mg_3N_2. The F 1s spectrum (Fig. 4e) yields at the surface two main bonding states with binding energies 685.3 eV and 683.2 eV attributed to the Mg-F bond in MgF_2 and the Al-F bond in AlF_3, respectively.

Based on the above XPS analysis results, we concluded that AlF_3 and AlN phases existed in the surface films on all the conversion times. However, because the amount of these compounds were much less than that of other compounds, such as MgF_2, these phases were not detected in the X-Ray analysis.

Therefore, increasing the conversion time favoures the diffusion processes that are associated with the formation and growth of secondary phases. These phases are not always desirable because they may adversely affect the corrosion resistance of these generated layers.

Aside from what is expected, an increase of the exposure time will not allow a better corrosion resistance, because the formation of a water soluble phase (AlF3) increases. On the other hand, at 30 min exposure the film formed is not enough to protect the sample from corrosion. Therefore a 60 min exposure will be the best option due to an adequate film thickness and a concentration of AlF3 that will not affect the corrosion resistance. In addition, at 90 min exposure, the film could have overcome a limit thickness, which causes an increasing residual stress. These stresses could be responsible for layer cracking and the loss of continuity of the same decreasing this way of the corrosion resistance.

The coatings produced have different morphological and compositional characteristics, which will significantly influence in their protective behaviour. Thus, polarization curves were carried out to investigate the influence of the conversion time on the corrosion resistance of the produced coatings. The polarization curves of the AZ91D and coated-AZ91D samples are shown in Fig. 5.

The polarization curves are fitted and the corresponding Tafel data are shown in Table 2. The corrosion potential, E_{corr}, of coated samples, measured at the intersection between the anodic and cathodic slopes, was relatively constant at -1.5 $V_{Ag/AgCl}$ and the coated samples exhibited a higher corrosion potential than the un-coated alloy. The rise in corrosion potential of the coated samples can be associated with an improvement of the integral coating, while a drop can be due to the film rupture. The formation of the film improving the

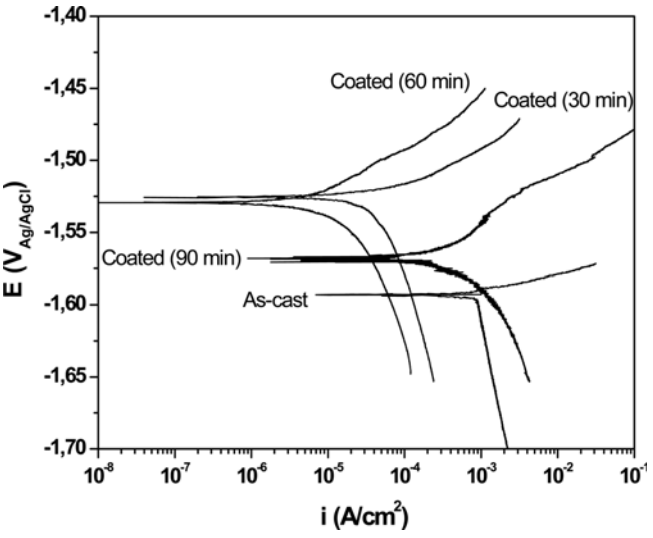

Fig. 5. Polarization curves of un-coated and coated AZ91D magnesium alloy in 3.5 wt% NaCl aqueous solution.

Table 2. Polarization data of tested samples in 3,5 wt% NaCl, as a function of conversion time in N_2/HFC-134a

Sample	Time (min)	E_{corr} (V)	I_{corr} (A/cm^2)	Rp (Ωcm^2)
Un-coated AZ91D	0	-1.59	$7.9 \cdot 10^{-4}$	37.25
Coated AZ91D	30	-1.52	$3.4 \cdot 10^{-5}$	2431.91
	60	-1.53	$8.7 \cdot 10^{-6}$	4794.75
	90	-1.56	$5.2 \cdot 10^{-4}$	159.84

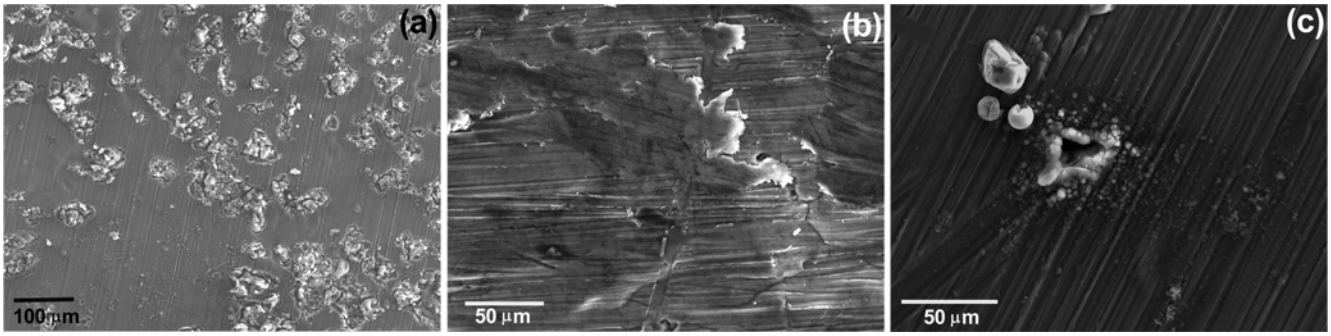

Fig. 6. SEM surface micrographs after potentiodynamic polarization test of: (a) un-coated AZ91D magnesium alloy; (b) coated AZ91D alloy obtained for 30 min of conversion time, and (c) coated AZ91D alloy obtained for 90 min of conversion time.

corrosion resistance of the coated samples takes place as a consequence of the interaction of F with Mg and Al.

The cathodic polarization curve shifts to left for coated samples obtained at 30 and 60 min, indicating the inhibition of the reduction of hydrogen in these cases. However, the cathodic curve for the coating obtained at a longer time presents a similar trend to that of the un-coated alloy. The corrosion current density was also calculated directly from the polarization curves by Tafel region extrapolation from the polarization curves. We found that the corrosion density of the coated samples decreased with an increasing conversion time (up 60 min) from $7.9 \cdot 10^{-4}$ A cm^{-2} to $8.7 \cdot 10^{-6}$ A cm^{-2} by about two orders of magnitude, compared with the un-coated samples, which indicates that the coating generated on the surface decreased the corrosion rate of the un-coated AZ91D alloy.

These behaviours can be associated with the nature and composition of the coating obtained by chemical conversion. The un-coated sample presents a surface film of MgO which formed on the substrate by reaction with atmospheric oxygen. However, the coated samples present films composed mainly of fluorides. The corrosion rate increases for the coated samples obtained at a long conversion time. This fact can be due to the existence of a greater amount of aluminium fluoride in the coatings, which can be formed as consequence of the diffusion processes. This phase has a high solubility in water, so that its dissolution may cause pitting during the electrochemical measurements, thus increasing the corrosion rate.

The corrosion morphologies of the corroded specimens are shown in Fig. 6. The difference in polarization resistances is caused by a difference in the microstructure, composition and quantity of surface products formed on the surface of the samples. On the surface of the un-coated AZ91D alloy, the morphology of corrosion attack in chloride-containing media revealed localized corrosion at the α-Mg/β-$Mg_{17}Al_{12}$ interface (Fig. 6a). The separation between anodic (α-Mg phase) and cathodic zones (β-$Mg_{17}Al_{12}$ phase) is large and not effectively blocked either by the β-phase or by the corrosion products deposited between the β-phase and the α-phase, causing the early pitting observed in AZ91 based specimen.

The coating obtained at short and medium conversion times has a good corrosion resistance, and local corrosion is not visible, which we attribute to its compact structure (Fig. 6b). Therefore, the continuity of the coating becomes more protective and inhibits anodic dissolution. Due to the existence of large pores in the outer films of the coating, the coating produced at a long time is not satisfying and it loses its protection effect on the AZ91D alloy (Fig. 6c).

4. CONCLUSIONS

We studied the influence of conversion time for the AZ91D magnesium alloy on N_2/HFC-134a atmospheres and drew the following conclusions.

(1) A protective film of MgF_2 formed on the AZ91D magnesium alloy surface in an atmosphere of N_2 containing a 2 wt.% HFC-134a at 550 ℃ for 60 min.

(2) An increase in the conversion time resulted in an increase in the continuity and compactness of the coating generated on the surface of the AZ91D alloy. However, the formation of a greater number of phases as AlF_3 at a long conversion time (90 min) caused discontinuity in the film because this phase is water soluble. Therefore, a 60 min exposure is the suitable time to find a balance between the formation of water soluble phases and film thickness.

(3) The corrosion density current of coated samples decreased by increasing the conversion time (up 60 min) by about two orders of magnitude, compared with the un-coated samples, which indicates that the coating generated on the surface decreased the corrosion rate of the un-coated AZ91D alloy.

ACKNOWLEDGEMENTS

The authors would like to thank the financial support provided by the projects MAT2010-20311 and Santander-UCM GR35/10-A.

REFERENCES

1. S. Anbu and S. Ramanathan, *Mater. Des.* **31**, 1930 (2010).
2. M. I. Barrena, J. M. Gómez de Salazar, L. Matesanz and A. Soria, *Mater. Charact.* **62**, 982 (2011).
3. E. Aghion and N. Lulu, *Mater. Charact.* **61**, 1221 (2010).
4. Y. Gu, X. Cai, Y. Guo, and C. Ning, *Mater. Design* **43**, 542 (2013).
5. L. Wang, T. Shinohara, and B. P. Zhang, *Mater. Design* **33**, 345 (2012).
6. L. Wang, B. P. Zhang, and T. Shinohara, *Mater. Design* **31**, 857 (2010).
7. H. Altun and S. Sen, *Mater. Design* **31**, 637 (2004).
8. N. I. Z. Abidin, D. Martin, and A. Atrens, *Corros. Sci.* **53**, 862 (2011).
9. T. Zhang, G. Meng, Y. Shao, Z. Cui, and F. Wang, *Corros. Sci.* 53, 2934 (2011).
10. B. Çiçek and Y. Sun, *Mater. Design* **37**, 369 (2012).
11. N. D. Nam, M. Z. Bian, M. Forsyth, M. Seter, M. Tan, and K. S. Shin, *Corros. Sci.* **64**, 263 (2012).
12. P. Li, M. K. Lei, and X. P. Zhu, *Mater. Charact.* **62**, 599 (2011).
13. Y. F. Jiang, L. F. Liu, C. Q. Zhai, Y. P. Zhu, and W. J. Ding, *Thin Solid Films* **484**, 232 (2005).
14. A. Scott and J. E. Gray-Munro, *Thin Solid Films* **517**, 6809 (2009).
15. S. Candan, M. Unal, E. Koc, Y. Turen, and E. Candan, *J. Alloy. Compd.* **509**, 1958 (2011).
16. X. Chen, G. Li, J. Lian, and Q. Jiang, *Surf. Coat. Tech.* **204**, 736 (2009).
17. X. F. Wang and S. M. Xiong, *Trans. Nonferr. Met. Soc. China* **21**, 807 (2011).
18. G. Pettersen, E. Øvrelid, G. Tranell, J. Fenstad, and H. Gjestland, *Mater. Sci. Eng. A* **332**, 285 (2002).
19. S. M. Xiong and X. F. Wang, *Trans. Nonferr. Met. Soc. China* **20**, 1228 (2010).
20. H. Chen, J. Liu, and W. Huang, *Corros. Sci.* **52**, 3639 (2010).
21. J. R. Liu, H. K. Chen, L. Zhao, and W. D. Huang, *Corros. Sci.* **51**, 129 (2009).
22. W. Ha and Y. J. Kim, *J. Alloy. Compd.* **422**, 208 (2006).
23. H. Chen, *Mater. Charact.* **61**, 894 (2010).
24. H. Chen, J. Liu, and W. Huang, *Mater. Charact.* **58**, 51 (2007).
25. H. Chen, J. Liu, and W. Huang, *J. Mater. Sci.* **41**, 8017 (2006).